Verhaegen et al.

SUPPLEMENTARY INFORMATION

Protein Immunoblots. Total cell lysates were obtained by Laemmli extraction and quantified by standard Bradford method using Bio-Rad Protein Assay dye reagent concentrate (Bio-Rad Laboratories, Hercules, CA). Protein samples were separated on 12% or 4-20% gradient SDS-polyacrylamide gels and transferred to Immobilon-P membranes (Millipore, Bedford, MA). Antibodies used are as follows: p53 (Clone CM1) from Novocastra (Newcastle-upon-Tyne, UK), phosphorylated p53-Serine 15 and Caspase-3 from Cell Signaling Technology (Danvers, MA), MDM2 (AB-1) from EMD Chemicals (San Diego, CA), green fluorescent protein (GFP) from Roche Applied Science, p16INK4A and Rb from BD Biosciences, p14ARF from Novus Biologicals (Littleton, CO), Mcl-1, p21, E2F-1 (KH95), and ubiquitin from Santa Cruz Biotechnology (Santa Cruz, CA). Anti-α-tubulin or anti-β-actin (Sigma-Aldrich, St. Louis, MO) were routinely included for loading controls. Protein expression was quantified using Scion image densitometry software (Scion Corporation, Frederick, MD).

SUPPLEMENTARY FIGURES

Supplementary TABLE 1. Cell lines used in this study. p53 mutational status was determined by direct sequencing of exons 2-10 by RT-PCR. Samples with polymorphism P72R are indicated as^{R}. The inducibility of p53 was determined by immunoblotting of extracts treated with adriamycin (0.5 μg/ml, 12h). Lines with high endogenous levels of p53 are indicated with an asterisk. B-RAF and N-Ras sequences at exon 15 and 3 respectively, were determined by direct sequencing of PCR-amplified genomic fragments. PTEN expression was analyzed by protein immunoblotting, and quantified using normal melanocytes as reference.

Supplementary FIGURE S1. Impact of p53 depletion in melanocytes and melanoma cell lines. *A*, visualization by immunoblotting of the endogenous levels of p53 in SK-Mel-103 after the indicated times post-infection with lentiviral vectors coding for scrambled

shRNA control (C-shRNA) or p53shRNA. Note the stability of the p53 downregulation at long times after transduction (i.e. day 16). This reduction of p53 was not accompanied by DNA damage as indicated by the absence of changes in phosphorylated histone 2AX (γ-H2AX). *B*, Micrographs showing the morphology of normal melanocytes and the indicated melanoma cell lines at day 3 or day 15 after infection with control- or MDM2-shRNA lentiviruses. While melanoma cells kept proliferating without obvious changes in cell morphology, melanocytes showed a progressive accumulation of multinucleated cell populations. C, Comparative analyses of cell cycle progression of the indicated cell populations untransduced or transduced with C-shRNA or p53 shRNA. The amount of cells in G1, S or G2/M phases of the cell cycle was determined by flow cytometry.

Supplementary FIGURE S2. Sustained inhibition of melanoma cell proliferation by Nutlin-3. (A) Quantification of cell number (trypan blue exclusion) of SK-Mel-103 incubated the presence of vehicle control or 5 μM Nutlin-3 for the indicated times. At day 4.5, treatment was removed and the ability of cells to recover was also estimated by cell counting. (B) SA-b-Gal staining of SK-Mel-103 treated with vehicle or 5 μM Nutlin-3 for 4.5 days and after a 5 day recovery period. Note that while Nutlin-3 treatment did not lead to an absolute cessation of cell proliferation, it did diminish cell proliferation to a significant extent.

Supplementary FIGURE S3. Senescence-like arrest by MDM2shRNA and Nutlin-3 treatment in melanoma cells but not in normal melanocytes. (A) Microphotographs of SK-Mel-103 treated with vehicle control, Nutlin-3 or transduced with MDM2 shRNA. (B) Absence of apoptotic features as measured by the analysis of caspase-9 processing by immunoblotting. The proteasome inhibitor bortezomib (Bor) is included as an example of a potent pro-apoptotic activator in these cells (Fernandez *et al.*, 2005). (D) Estimation of cell death by trypan blue exclusion at 48h after treatment with the indicated coumpounds. (D) Micrographs of normal melanocytes treated in parallel with the melanoma cells shown in (A). (E) Lack of SA-β-Gal activity in melanocytes treated with 5 μM Nutlin-3 under conditions that allow for the detection of senescence features upon transduction of the oncogene $BRAF^{V600E}$ (a well-known senescence inducer in these cells (Denoyelle *et al.*, 2006)).

Supplementary FIGURE S4. P53/p21 dependent bypass of Nutlin-3 driven melanoma cell senescence. Shown are microphotographs of isogenic series of SK-Mel-103 infected with lentiviral vectors coding for scrambled shRNA or shRNAs that target either p16, p21 or p53. At day 2 post-infection cells were treated with 5 μM Nutlin-3, and micrographed 56 h thereafter. Note the marked inhibition in cell number and the morphological change of control cells and the lack of effect of p16 depletion. Absence of p21, and particularly p53, abrogated the detrimental effects of Nutlin-3 on melanoma cells. Immunoblots showing the efficacy of the shRNAs used in this study are shown in Fig. 5E. Fig. 4B summarizes the kinetics of cell proliferation after Nutlin-3 treatment of the above indicated cell lines.

Supplementary FIGURE S5. Nutlin-3 treatment fails to deplete E2F-1 levels in normal melanocytes. Shown are immunoblots prepared from melanocytes either untreated (NT) or treated with vehicle, 5 μM Nutlin-3 or 1 μg/ml doxorubicin for the indicated times. Note the massive induction of MDM2 by Nutlin-3, and the concomitant accumulation of p53 and p21 upon treatment, with no downregulation of E2F-1.

Supplementary FIGURE S6. E2F-1 overexpression counteracts the senescence-like features induced by Nutlin-3 in melanoma cells. (A) Micrographs of SK-Mel-103 transduced with adenoviral vectors coding for GFP (control) or E2F-1 at a multiplicity of infection of 10 pfu (plate forming units). 24h after infection cells were treated with 5 μM Nutlin-3 for 30 or 50 h for the visualization of cell vacuolization and cell flattening (A) and SA-b-Gal staining (B). (C) Induction of p53, MDM2 and p21 after infection with control or E2F-1 adenovirus, and treatment vehicle or 5 μM Nutlin-3 for the indicated times.

REFERENCES

Denoyelle C, Abou-Rjaily G, Bezrookove V, Verhaegen M, Johnson TM, Fullen DR *et al* (2006). Anti-oncogenic role of the endoplasmic reticulum differentially activated by mutations in the MAPK pathway. *Nat Cell Biol* **8:** 1053-63.

Fernandez Y, Verhaegen M, Miller TP, Rush JL, Steiner P, Opipari AW, Jr. *et al* (2005). Differential regulation of noxa in normal melanocytes and melanoma cells by proteasome inhibition: therapeutic implications. *Cancer Res* **65:** 6294-304.

Verhaegen et al.
Supplementary Table I

Cell type/ line	p53	p53 induct	p14 (protein)	p16 (protein)	B-RAF (V599)	N-Ras (exon 3)	PTEN (protein)
Melanocytes	wt	+	+	-	wt	wt	+
SK-Mel-19	wt	+	+	-	mutant	wt	+
SK-Mel-28	L145R	-*	+++	+	mutant	wt	-
SK-Mel-29	wt	+	+	-	mutant	ND	+
SK-Mel-94	wt	+	+	+/-	mutant	wt	-
SK-Mel-103	wt^{R}	+	-	++	wt	Q61R	-
SK-Mel-147	wt^{R}	+	-	++	wt	Q61R	-
SK-Mel-173	wt^{R}	+	-	-	wt	wt	-/+
G-361	wt^{R}	+	-	-	wt/mutant	wt	-
Malme-3M	wt^{R}	+	-	-	wt/mutant	wt	+
UACC-62	wt	+	-	-	mutant	wt	-
UACC-257	wt^{R}	+	++	-	wt	wt	ND
WM-1366	Y220C	-*	++	-	wt	Q61R	ND

Verhaegen et al.
Supplementary Figure S1

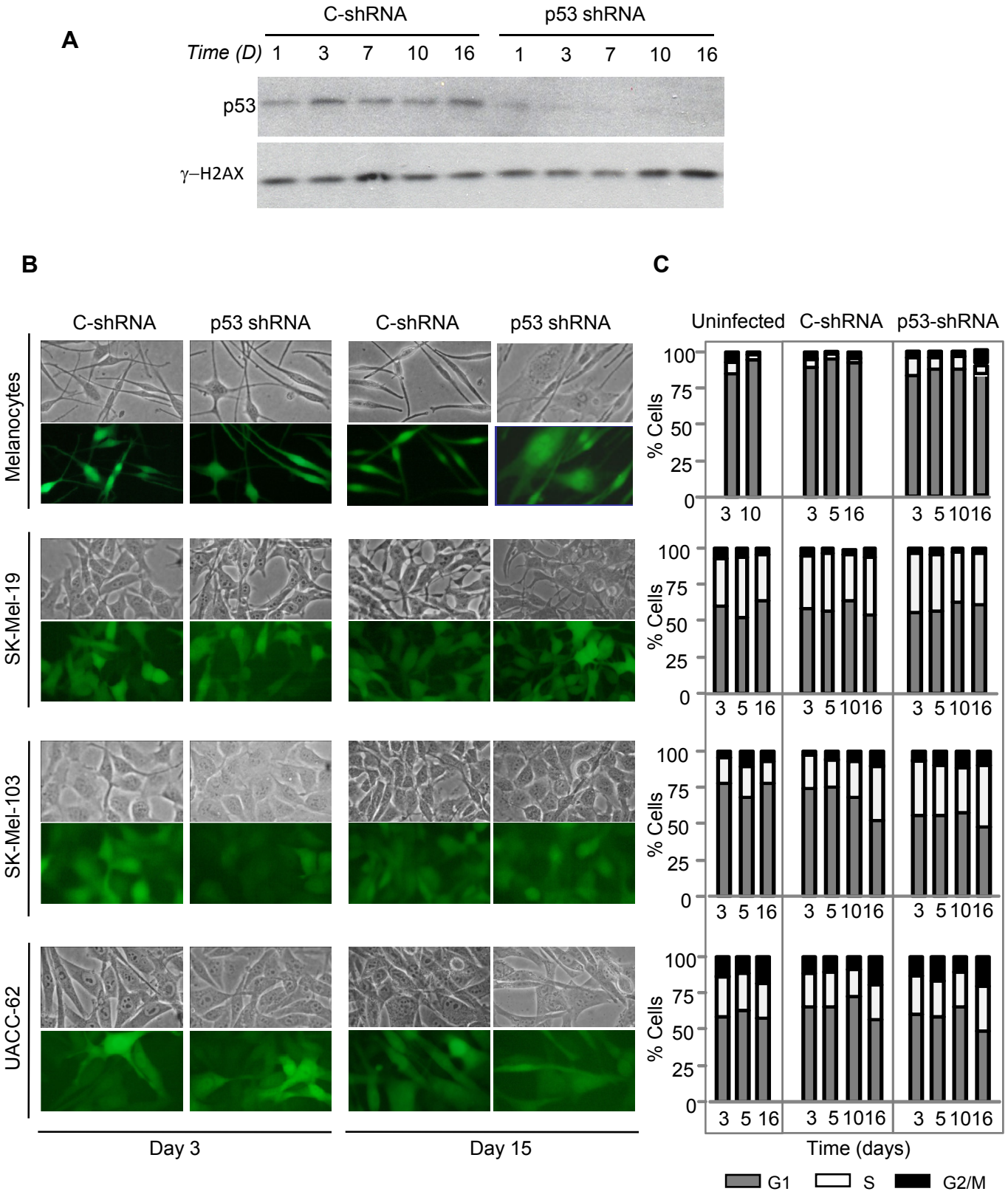

Verhaegen et al.
Supplementary Figure S2

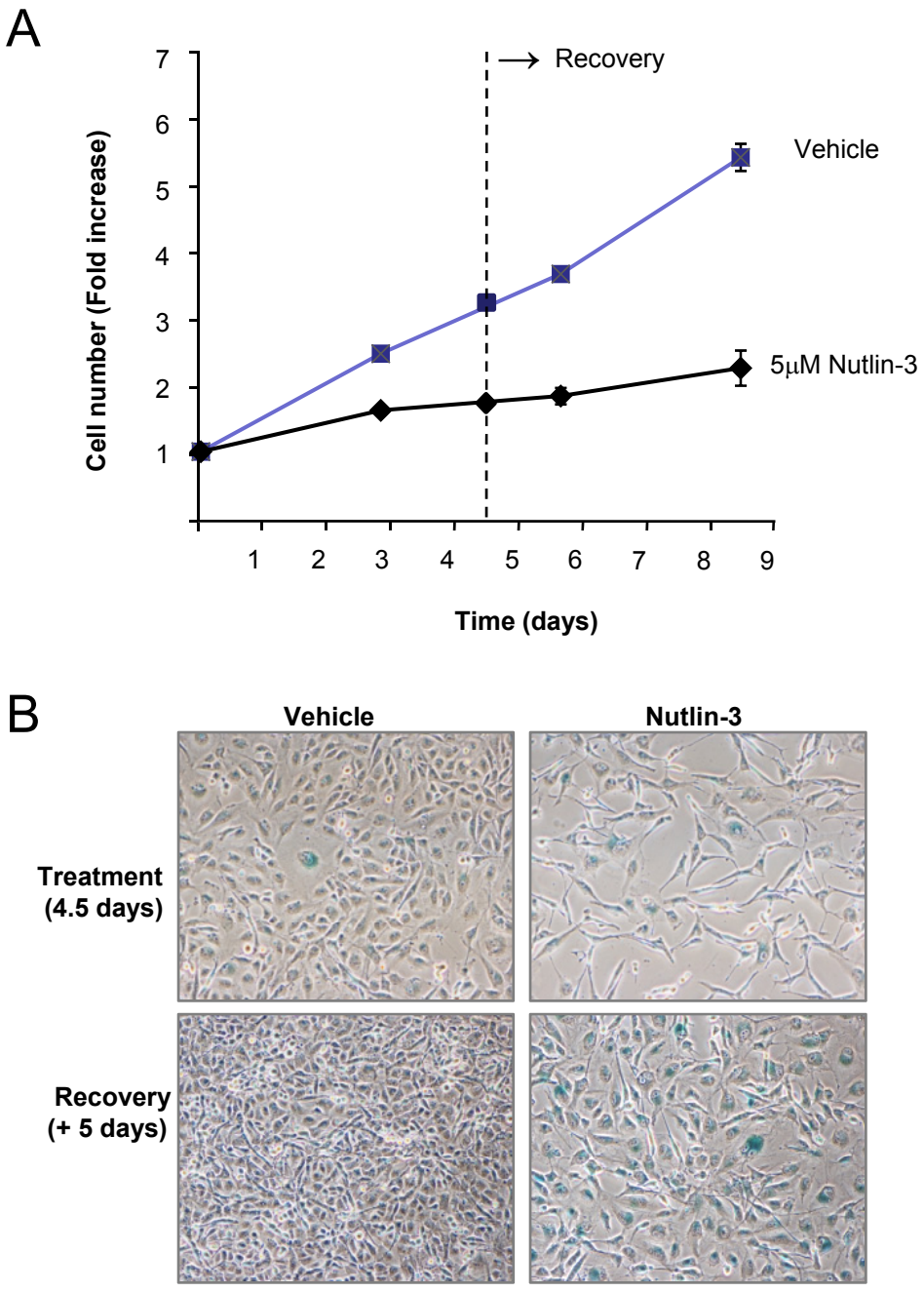

Verhaegen et al.
Supplementary Figure S3

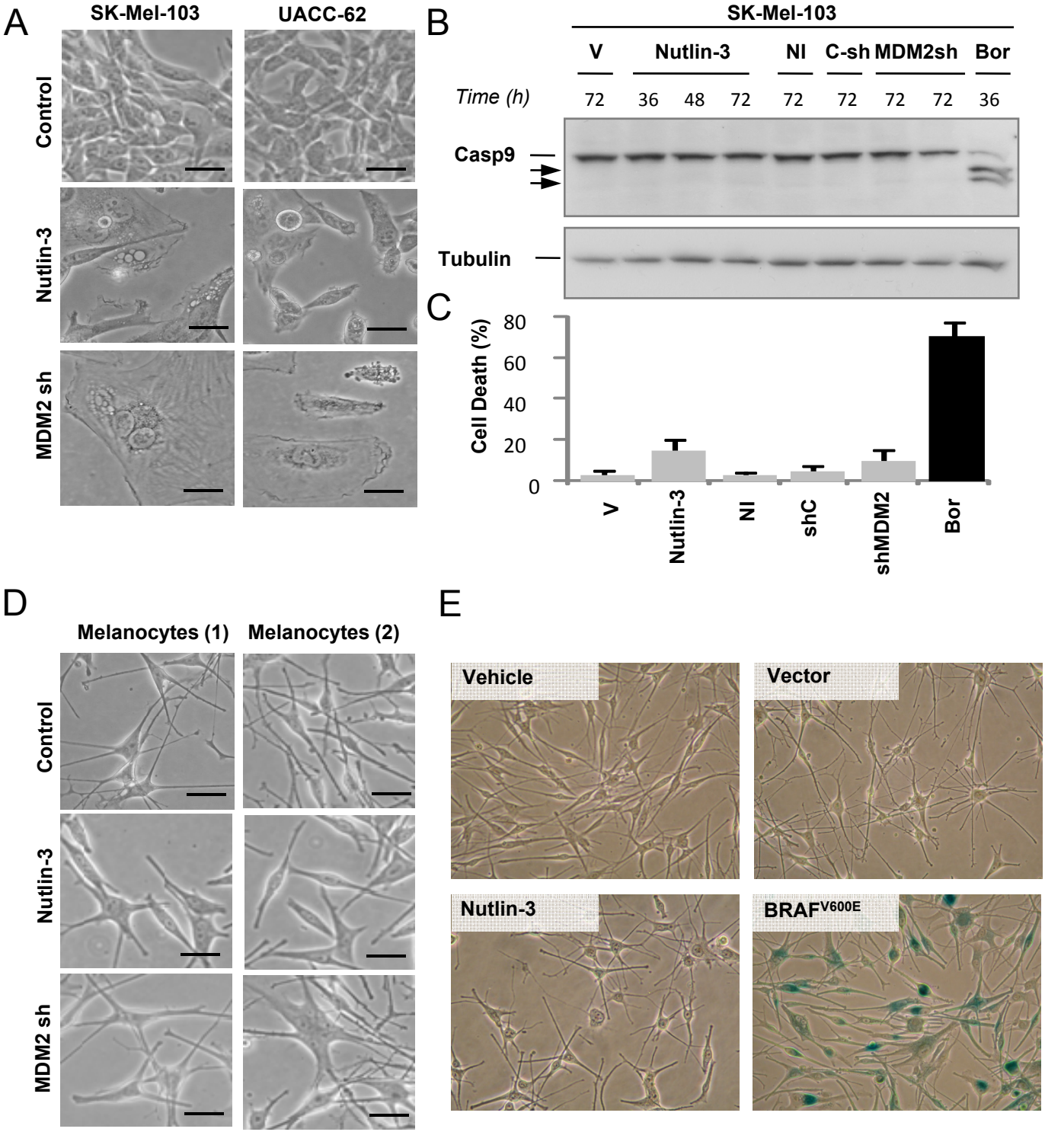

Verhaegen et al.
Supplementary Figure S4

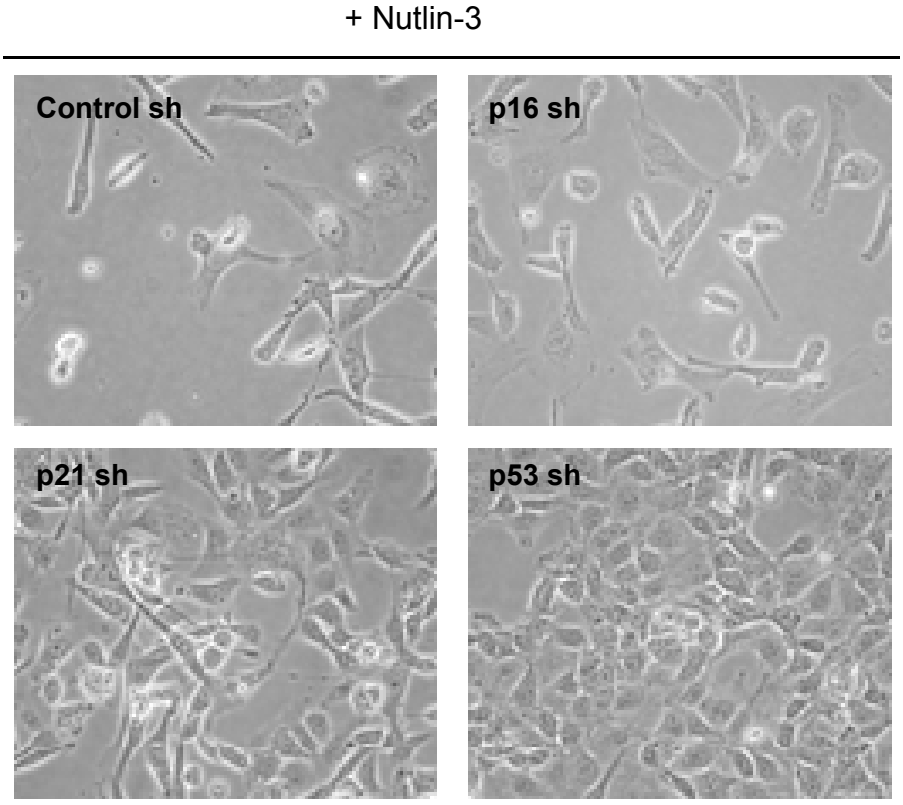

Verhaegen et al.
Supplementary Figure S5

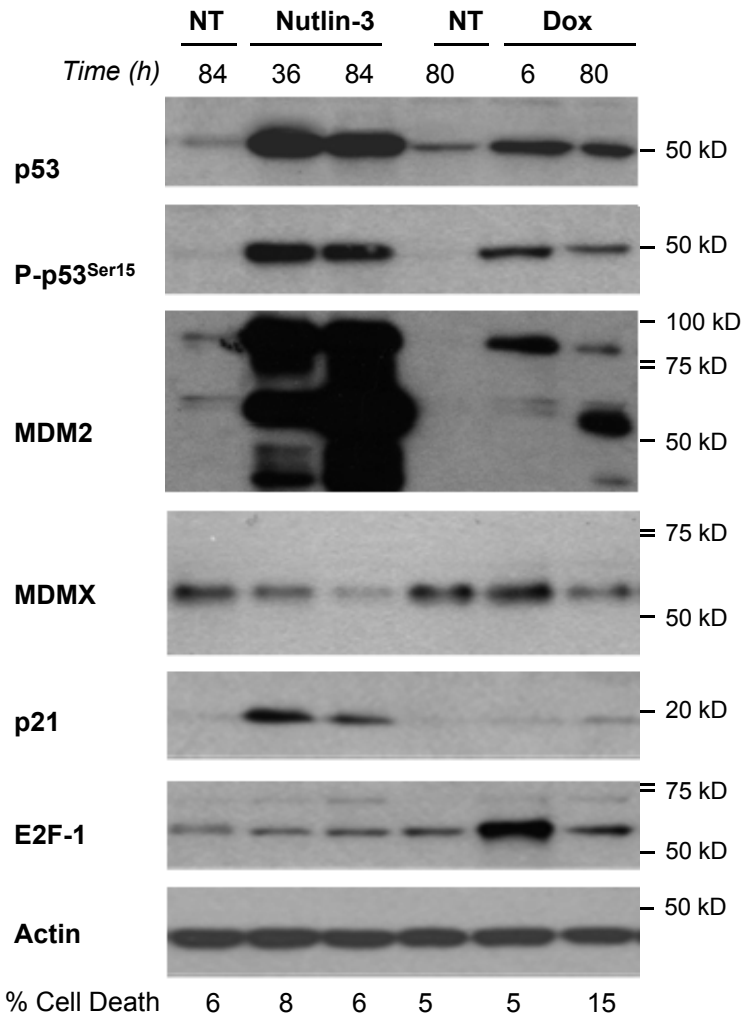

Verhaegen et al.
Supplementary Figure S6